Transactions National Academy of Science & Technology Philippines
ISSN 0115-8848 (print)
ISSN 2815-2042 (online)
Vol. 43 (2021)
doi.org/10.57043/transnastphl.2021.1799

Density, Refractive Index, and Viscosity Data of Aqueous Solutions of *n*-Tris(hydroxymethyl)methyl-3-aminopropanesulfonic Acid (TAPS)

Jennifer Kate I. Pailma,[1] Meng-Hui Li[2], Allan N. Soriano[3,*]

[1]School of Chemical, Biological, and Materials Engineering and Sciences, Mapúa University, Manila, 1002, Philippines
[2]R&D Center for Membrane Technology and Department of Chemical Engineering, Chung Yuan Christian University, Chung Li, 32023, Taiwan, R.O.C.
[3]Chemical Engineering Department, Gokongwei College of Engineering, De La Salle University, 2401 Taft Avenue, Manila, Philippines

ABSTRACT

Property characterization plays an important role in the design of processes and operations. Correlating the physical and chemical properties with key process parameters such as temperature and composition leads to the understanding of the systems behaviour. Thus, in this work, properties including density, refractive index, and viscosity data of aqueous solutions of *n*-tris(hydroxymethyl) methyl-3-aminopropanesulfonic acid (TAPS) were measured at varied temperature and fixed pressure. The considered temperatures and pressure were from 293.15 to 343.15 K and at atmospheric pressure, respectively. The compositional range studied was the entire composition range where TAPS was still soluble in water. The experimental data were correlated using a modified form of the Vogel-Tamman-Fulcher equation leading to an Arrhenius-type asymptotic exponential function. In general, the data presented together with the proposed correlation were of sufficient accuracy with an overall AAD value of 0.27%. Excess properties were also computed to account for the deviations of the solution from ideality.

*Email: allan.soriano@dlsu.edu.ph

Keywords:
Density;
Excess properties;
n-Tris(hydroxymethyl)methyl-3-amino-propanesulfonic acid; Refractive Index;
Viscosity;
Vogel-Tamman-Fulcher equation

Citation:
Pailma JKE, Li M-H, Soriano AN. 2021. Density, refractive index, and viscosity data of aqueous solutions of n-Tris(hydroxymethyl)methyl-3-aminopropanesulfonic acid (TAPS). Transactions NAST PHL 43(2): doi.org/10.57043/transnastphl.2021.1799

Transactions NAST PHL 43 (2021)
doi.org/10.57043/transnastphl.2021.1799

I. INTRODUCTION

Many chemical processes are markedly impaired by even small changes in the concentrations of free hydrogen ions (H^+). Biological systems rely upon chemical interactions between life-sustaining biomolecules and water. The biochemical properties of biomolecules depend upon the presence of chemical moieties which supply a positive or negative charge to the molecules and allow them to interact with the ionizable components of water. It is therefore necessary to stabilize the H^+ concentration by adding a suitable buffer to the medium without affecting the function of the system under investigation (Soriano et al. 2011; Taja and Lee 2009a; Taja and Lee 2009b). A buffer keeps the pH of the solution constant by taking up protons that are released during reactions or by releasing protons when they are consumed by reactions (Machado and Soares 2007). However, the choice of a pH buffer may constitute an important problem since many of them exhibit various deviations from the requirements of being inert and may disturb the equilibrium state (Machado et al. 2007).

The introduction of zwitterionic buffers seems to solve the problem and satisfy all the criteria for a perfect buffer. Zwitterionic buffers, by definition, contain both positive and negative ionizable groups (Taja and Lee 2010a; Palasz et al. 2008). Secondary and tertiary amines provide the positive charges, while sulfonic and carboxylic acid groups provide the negative charges. The nature of zwitterionic buffers makes them particularly suitable for various applications because they are very soluble in water. In addition, they can maintain a stable physiological pH range between 6.5 and 8.0 at a wide range of temperatures (Civan 2008; Roy et al. 2006).

In the selection of buffer substances for biochemical interest, TAPS is recognized. The reduced ion effect observed with TAPS buffer allows the preparation of solutions from concentrated stocks with minimal pH effects from the dilution of buffer components. Since TAPS has hydroxyl groups, a number of biological systems are found to be compatible while expressing better chemical stability and improved solubility. With such good qualities, TAPS is used in various biochemical applications, such as in capillary electrophoresis to analyze DNA, in planar chromatography to separate dyes, in dinoflagellate experiments as culture media buffer since it allows minimal pH change and maximal growth, and in inhibiting the connexin channels in animal cells (Gold Biotechnology 2021).

Many significant applications of TAPS require a thorough knowledge of its thermophysical properties. Despite this need, the necessary experimental data for many properties are scarce (Rooney et al. 2009). In literature, there are only those that work on the binary solutions containing TAPS and different glycols (De Jesus et al. 2013) and on the ternary systems containing aqueous solutions of TAPS with different glycols (De Jesus et al. 2020). Therefore, to realize the full potential of TAPS, this research measured its density, refractive index, and viscosity in an aqueous solvent system. These properties are determined for temperatures up to 343.15 K at atmospheric pressure and the entire composition range from 0.001 to 0.007 mole fractions. An Arrhenius-type asymptotic exponential function from the modification of the Vogel-Tamman-Fulcher equation was used to generally correlate the temperature and compositional dependence of the considered properties.

II. MATERIAL AND METHODS

2.1 Chemicals

The TAPS buffer acquired was reagent grade with minimum mass fraction purity of 0.9999 from MP Biomedicals, Inc. It was used without further purification. The liquid water used to prepare the aqueous solutions was a Type I reagent grade deionized water with a resistivity of 18.3 MΩ·cm and total organic carbon content of less than $15 \cdot 10^{-9}$ and produced via Barnstead Thermodyne (model Easy Pure 1052) water purification system. A Mettler-Toledo (model AL204) digital balance having an accuracy of $\pm 1 \cdot 10^{-4}$ g was used in the preparation of the aqueous buffer solutions. The prepared solutions were degassed for up to 1 h

Transactions NAST PHL 43 (2021)
doi.org/10.57043/transnastphl.2021.1799

using the ULVAC vacuum pump from SINKU KIKO (model GVD-050A).

2.2 Property Measurements

Prior to the measurements of the system studied, available literature data for the density, refractive index, and viscosity of deionized water were considered first. The calibration was done to ensure that the applied procedures and apparatus for each property measurement could provide accurate results throughout the reportable range.

All measurements were carried out in three to five replicate runs and the average values were reported. The thermophysical property measurements for the considered binary solutions were measured as follows:

Density (ρ). The density of the solutions was measured in triplicate through the SVM 3000 Stabinger density measuring cell having an uncertainty of $\pm 4 \cdot 10^{-4}$ g·cm^{-3}. The density meter used the principle of oscillating U-tube (Graber et al. 2004; Wong et al. 2008). The sample is introduced into a U-shaped tube that is electronically excited to oscillate at its characteristic frequency. The characteristic frequency changes depending on the density of the sample. Through the precise determination of the characteristic frequency and an appropriate adjustment, the density of the sample is determined. But, due to the high-temperature dependency of the density, the measuring cell has to be accurately thermostatted. For each concentration, 5 mL was placed in a syringe, and 1.5 mL of it was used per trial. The repeatability of the density measurement was ±0.0002 g·cm^{-3} and the estimated uncertainty for temperature was ±0.002 K.

Refractive index (n_D). The refractive index of each solution was measured in triplicate using an Abbemat WR-MW digital refractometer having an uncertainty of $\pm 4 \cdot 10^{-5}$. It consisted of an internal solid-state Peltier thermostat and two internal Pt-100 Platinum resistance temperature sensors for exact temperature measurement. Through these features, exact temperature measurements were assured. For each trial, 1 mL of the sample was used in the experiment. A total of 3 mL per sample was used in the experiment. The refractometer finds the critical angle of an incident beam of monochromatic light. Here the sample to be measured is placed on the polished surface of a prism made of synthetic YAG, a hard scratchproof and corrosion-resistant material. A cone-shaped yellow light beam of 589.3 nm sodium D wavelength illuminates the sample from its bottom side under a different angle of reflection. Then a microprocessor calculates the refractive index of the sample from the obtained data. The estimated uncertainties for temperature and refractive index were ±0.03 K and, $\pm 5 \cdot 10^{-5}$, respectively.

Viscosity (μ). The viscosities of the solutions were measured with an AMVn-automated micro viscometer, which is according to Höppler's falling ball principle. A ball rolls through a closed liquid-filled capillary, which is inclined at a defined angle. Two inductive sensors determine the ball's rolling time between two defined marks. Both the liquid's dynamic and kinematic viscosity can be calculated from the rolling time. The uncertainties of the measured temperature and viscosity were estimated to be ±0.05K and ±1.0%, respectively.

2.3 Measurements' Validation

When setting up the system for analysis, it is necessary to validate the measurement methodologies for the investigated properties. The calibration and certain sampling precautions are key factors in determining the robustness of the method and, as a rule, extra care taken at this stage is easily paid back in terms of the reliability of the final method. For this study, it was found adequate to use deionized water, spanning the same temperature range. Calibration details are shown in Table 1. The property measurements of water from this work are in good agreement with the available data in the literature. Such results are quantitatively evaluated via the average percentage deviation (APD). The overall APD for the three properties is 0.27%, which is very satisfactory, thus validating the present experimental procedures and the apparatus used.

Transactions NAST PHL 43 (2021)
doi.org/10.57043/transnastphl.2021.1799

Table 1. Comparison of thermophysical properties (ρ, η, μ) of the systems used for measurement calibration.

T/K	ρ / g·cm^{-3}		η_D / dimensionless		μ / mPa·s	
	Geankoplis (1993)	This work	Schiebener and Straub (1990)	This work	NIST (2021)	This work
293.15	0.99823	0.99883	1.33336	1.33299	1.00160	1.00503
298.15	0.99708	0.99783	1.33283	1.33244	0.89008	0.89223
303.15	0.99568	0.99650	1.33230	1.33186	0.79735	0.80050
313.15	0.99225	0.99327	1.33095	1.33048	0.65298	0.65267
323.15	0.98807	0.98923	1.32937	1.32883	0.54685	0.54993
333.15	0.98324	0.98457	1.32757	1.32694	0.46640	0.46640
343.15	0.97781	0.97917	1.32559	1.32487	0.40389	0.40389
APD[a]	0.10		0.04		0.57	

[a] $\text{APD}/\% = \frac{100}{n} \cdot \sum_{i=1}^{n} |(\text{Ref} - \text{Expt})/\text{Ref}|_i$, where n is the number of data points

III. RESULTS AND DISCUSSION

Tables 2 to 4 show the experimental values obtained for ρ, η_D, and μ for the system studied as a function of the temperature and concentration, where x_i represents the mole fractions of TAPS. These data sets are also representatively shown in Figures 1 to 3. As seen in these figures, the density, refractive index, and viscosity always decrease with increasing temperature. The dependency of the three properties on concentration at a given temperature can also be noted since they all increase with increasing TAPS concentration. In interpreting the plots shown, it is by virtue of the sulfonic group, protonated amine, and hydroxyl groups of buffers that it interacts mainly through hydrogen-bonding (Lee and Taja 2010b). It must be noted that the intermolecular interactions become weaker with an increase in temperature.

Table 2. Specific densities of the {TAPS (1) + H_2O (2)} system.

T / K	ρ / g·cm^{-3}						
	x_1=0.001	x_2=0.002	x_3=0.003	x_4=0.004	x_5=0.005	x_6=0.006	x_7=0.007
293.15	1.00393	1.00873	1.01390	1.01880	1.02320	1.02747	1.03220
298.15	1.00290	1.00767	1.01283	1.01773	1.02207	1.02633	1.03097
303.15	1.00157	1.00627	1.01140	1.01627	1.02030	1.02480	1.02957
313.15	0.99810	1.00280	1.00807	1.01293	1.01720	1.02110	1.02607
323.15	0.99310	0.99763	1.00337	1.00877	1.01257	1.01643	1.02187
333.15	0.98563	0.99223	0.99733	1.00293	1.00780	1.01147	1.01610
343.15	0.97637	0.98387	0.98897	0.99513	1.00090	1.00490	1.00907

Transactions NAST PHL 43 (2021)
doi.org/10.57043/transnastphl.2021.1799

Table 3. Refractive indices of the {TAPS (1) + H_2O (2)} system.

T / K	η_D / dimensionless						
	x_1=0.001	x_2=0.002	x_3=0.003	x_4=0.004	x_5=0.005	x_6=0.006	x_7=0.007
293.15	1.33501	1.33703	1.33891	1.34092	1.34297	1.34445	1.34614
298.15	1.33450	1.33655	1.33841	1.34038	1.34243	1.34395	1.34590
303.15	1.33394	1.33594	1.33780	1.33978	1.34185	1.34337	1.34535
313.15	1.33250	1.33456	1.33642	1.33840	1.34047	1.34196	1.34400
323.15	1.33089	1.33301	1.33486	1.33684	1.33904	1.34055	1.34274
333.15	1.32915	1.33125	1.33308	1.33515	1.33754	1.33915	1.34144
343.15	1.32696	1.32917	1.33097	1.33331	1.33580	1.33758	1.34022

Table 4. Viscosities of the {TAPS (1) + H_2O (2)} system.

T / K	μ / mPa·s						
	x_1=0.001	x_2=0.002	x_3=0.003	x_4=0.004	x_5=0.005	x_6=0.006	x_7=0.007
293.15	1.33501	1.33703	1.33891	1.34092	1.34297	1.34445	1.34614
298.15	1.33450	1.33655	1.33841	1.34038	1.34243	1.34395	1.34590
303.15	1.33394	1.33594	1.33780	1.33978	1.34185	1.34337	1.34535
313.15	1.33250	1.33456	1.33642	1.33840	1.34047	1.34196	1.34400
323.15	1.33089	1.33301	1.33486	1.33684	1.33904	1.34055	1.34274
333.15	1.32915	1.33125	1.33308	1.33515	1.33754	1.33915	1.34144
343.15	1.32696	1.32917	1.33097	1.33331	1.33580	1.33758	1.34022

It is useful to consider temperature to be a measure of the kinetic energy of all atoms and molecules in a given system. As temperature increases, there is a corresponding increase in the vigor of translational and rotational motions of all molecules, as well as the vibrations of atoms and groups of atoms within molecules. Intermolecular forces vary considerably and the thermophysical property of a compound is a measure of the strength of these forces. Thus, to break the intermolecular attractions that hold the molecules of a compound, it is necessary to increase their kinetic energy by raising the sample temperature.

Transactions NAST PHL 43 (2021)
doi.org/10.57043/transnastphl.2021.1799

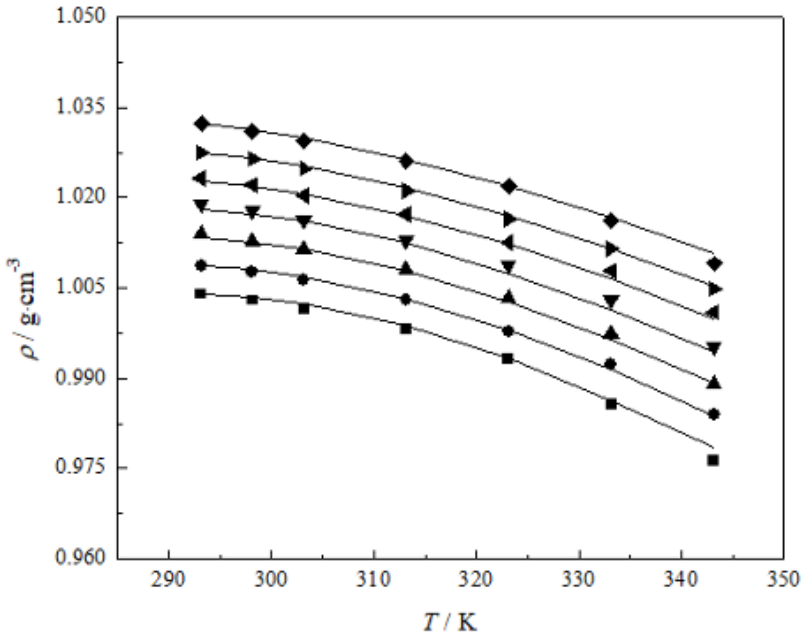

Figure 1. Plot of the Density Data for the {TAPS (1) + H_2O (2)} System as a Function of Temperature: ■, x_1 = 0.001; ●, x_2 = 0.002; ▲, x_3 = 0.003; ▼, x_4 = 0.004; ◄, x_5 = 0.005; ►, x_6 = 0.006; ♦, x_7 = 0.007; and Lines, Calculated Using Equation (2).

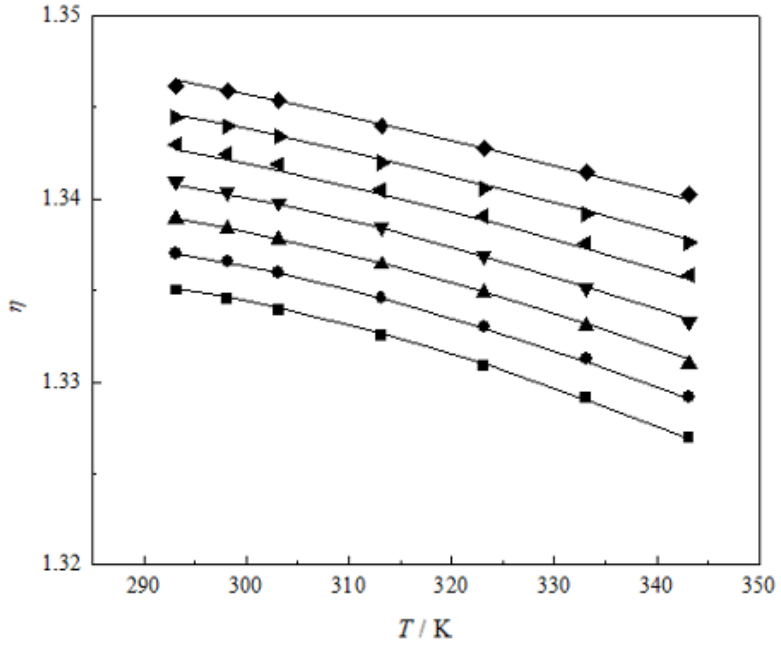

Figure 2. Plot of the Refractive Index Data for the {TAPS (1) + H_2O (2)} System as a Function of Temperature: ■, x_1 = 0.001; ●, x_2 = 0.002; ▲, x_3 = 0.003; ▼, x_4 = 0.004; ◄, x_5 = 0.005; ►, x_6 = 0.006; ♦, x_7 = 0.007; and Lines, Calculated Using Equation (2).

Transactions NAST PHL 43 (2021)
doi.org/10.57043/transnastphl.2021.1799

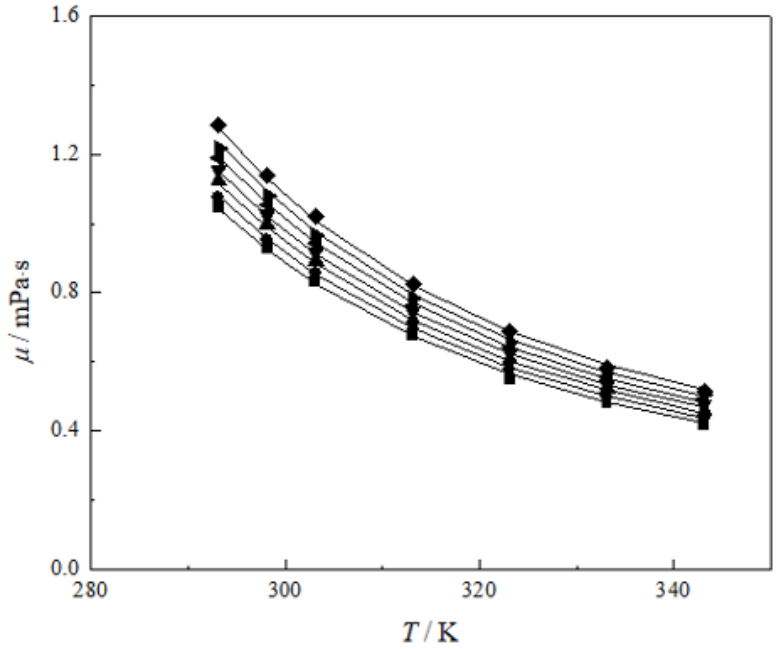

Figure 3. Plot of the Viscosity Data for the {TAPS (1) + H_2O (2)} System as a Function of Temperature: ■, x_1 = 0.001; ●, x_2 = 0.002; ▲, x_3 = 0.003; ▼, x_4 = 0.004; ◄, x_5 = 0.005; ►, x_6 = 0.006; ♦, x_7 = 0.007; and Lines, Calculated Using Equation (2).

The density, refractive index, and viscosity values are correlated by employing a modified form of the Vogel-Tamman-Fulcher (VTF) equation. This leads to an Arrhenius-type asymptotic exponential function with the addition of a second-order term.

$$\ln y = \ln(y_c) - \frac{A_1}{T} + \frac{A_2}{T^2} \qquad (1)$$

Equation (1) presents the expression for the three properties mentioned where y is the temperature-dependent property, y_C is the pre-exponential coefficient, T is the system temperature, and A is the constant incorporating the activation energy of the process.

Applying the considered property, Equations (2) and (3) were derived where A_i are the empirical parameters and x_1 is the mole fraction of TAPS in the solution.

$$y = \exp\left[A_0 + \frac{A_1}{(T/K)}\right] \qquad (2)$$

$$A_i = a_{i,0} + a_{i,1}(x_1) + a_{i,2}(x_1)^2 \qquad (3)$$

The empirical parameters ($a_{i,0}$, $a_{i,1}$, $a_{i,2}$) for each property were determined by fitting the values of the measured property using Equation (2).

The absolute average deviations (AAD) between the calculated and experimental values are presented in Table 5 and the parameters determined for the considered properties are listed in Table 6. Figures 1 to 3 compare the values of the three properties obtained by the VTF equation (solid lines) with the experimental values obtained for the TAPS + H_2O system. The calculated values are in good agreement with the experimentally obtained values.

Transactions NAST PHL 43 (2021)
doi.org/10.57043/transnastphl.2021.1799

Table 5. Calculated results for the properties of the {TAPS (1) + H_2O (2)} system using Equation (2).

Thermophysical property	*T* range/K	x_1 range	No. of data points, *n*	AAD[a] / %
ρ	293.15 to 343.15	0.001 to 0.007	49	0.05
ηD	293.15 to 343.15	0.001 to 0.007	49	0.01
μ	293.15 to 343.15	0.001 to 0.007	49	0.75
Overall			147	0.27

[a] $\text{AAD/\%} = \frac{100}{n} \cdot \sum_{i=1}^{n} |(\text{Cald} - \text{Expt})/\text{Expt}|_i$

Table 6. Parameters of Equation (2) for the considered properties of the {TAPS (1) + H_2O (2)} system.

Thermophysical property	Parameters			
	i	$a_{i,0}$	$a_{i,1}$	$a_{i,2}$
ρ	0	-1.2430	79.685	728.17
	1	-4.5929×10^{4}	-1.0671×10^{5}	7.0163×10^{6}
ηD	0	0.090820	16.746	110.19
	1	-9234.8	-1.5389×104	1.3892×106
μ	0	0.72957	145.96	-2582.6
	1	-7.1773×10^{4}	6.9525×10^{5}	1.1367×10^{8}

The excess properties provide a convenient way for measuring how a real mixture deviates from an ideal solution. To evaluate these properties, the real and the ideal fluid are considered under the same conditions of temperature and pressure.

$$E = Mixture - \left(x_1 S_1^0 + (1 - x_1) S_2^0\right) \qquad (4)$$

Equation (4) shows the general equation for excess properties where *E* is the excess property, x_1 is the mole fraction of one pure component; S_1 and S_2 are the considered properties of the pure components.

In Figure 4, the behavior of excess densities is quite complex. Figures 5 and 6 show a positive trend for the excess refractive indices and a negative trend for the excess viscosities, respectively. These changes in excess properties reflect complex and subtle changes in the effects of molecular interactions in response to the change in temperature. It is likely the competitive hydrogen bonding that is responsible for the relatively complex behavior of the excess properties through specific interactions between sulfonic, amino, and hydroxyl groups of TAPS buffer.

Transactions NAST PHL 43 (2021)
doi.org/10.57043/transnastphl.2021.1799

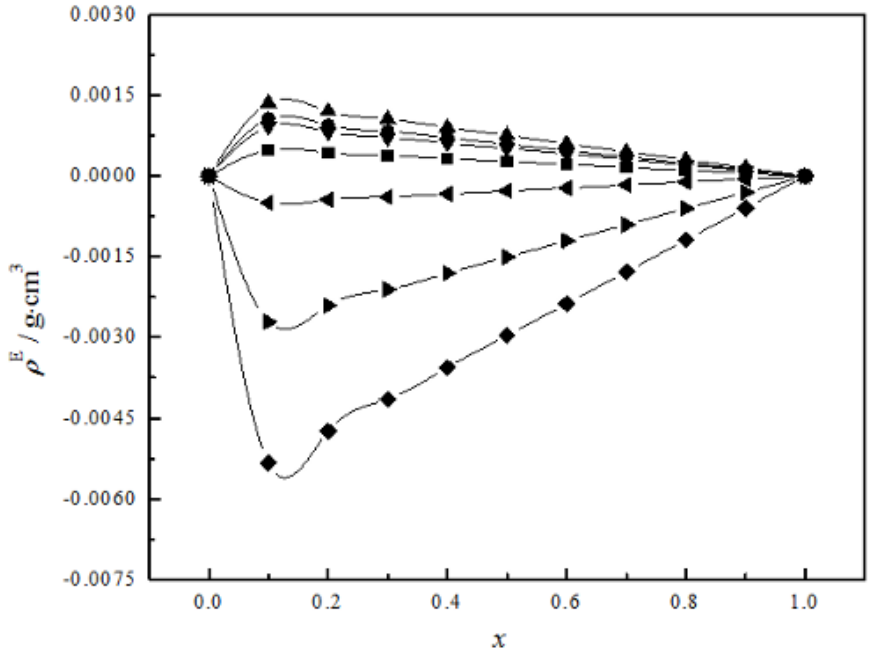

Figure 4. Plot of the excess density data for the {TAPS (1) + H2O (2)} system as a function of composition: ■, T_1 = 293.15 K ; ●, T_2 = 298.15 K; ▲, T_3 = 303.15 K; ▼, T_4 = 313.15 K; ◄, T_5 = 323.15 K; ►, T_6 = 333.15 K; ♦, T_7 = 343.15 K; and Lines are guide for the eyes.

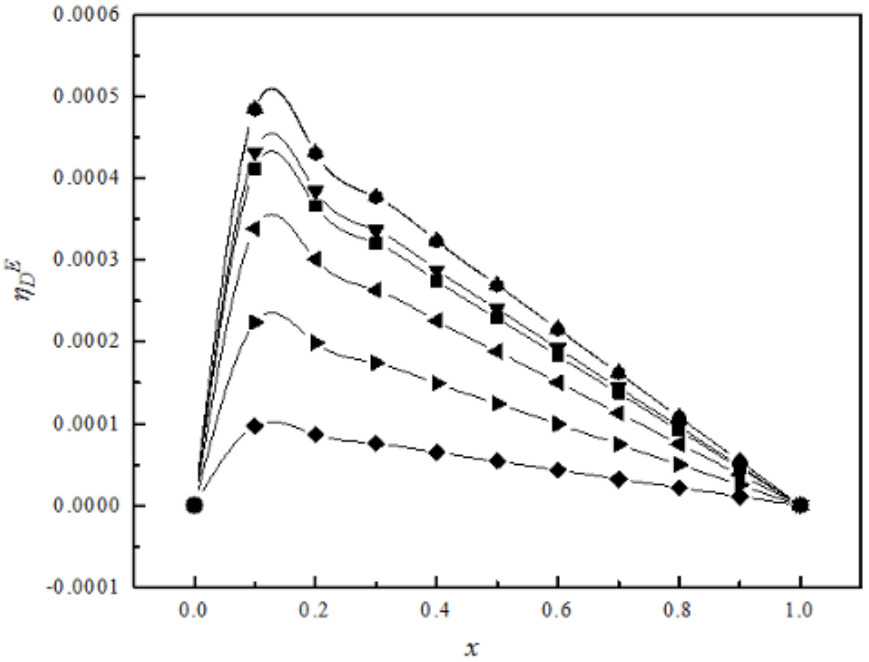

Figure 5. Plot of the excess refractive index data for the {TAPS (1) + H_2O (2)} system as a function of composition: ■, T_1 = 293.15 K ; ●, T_2 = 298.15 K; ▲, T_3 = 303.15 K; ▼, T_4 = 313.15 K; ◄, T_5 = 323.15 K; ►, T_6 = 333.15 K; ♦, T_7 = 343.15 K; and Lines are guide for the eyes.

Transactions NAST PHL 43 (2021)
doi.org/10.57043/transnastphl.2021.1799

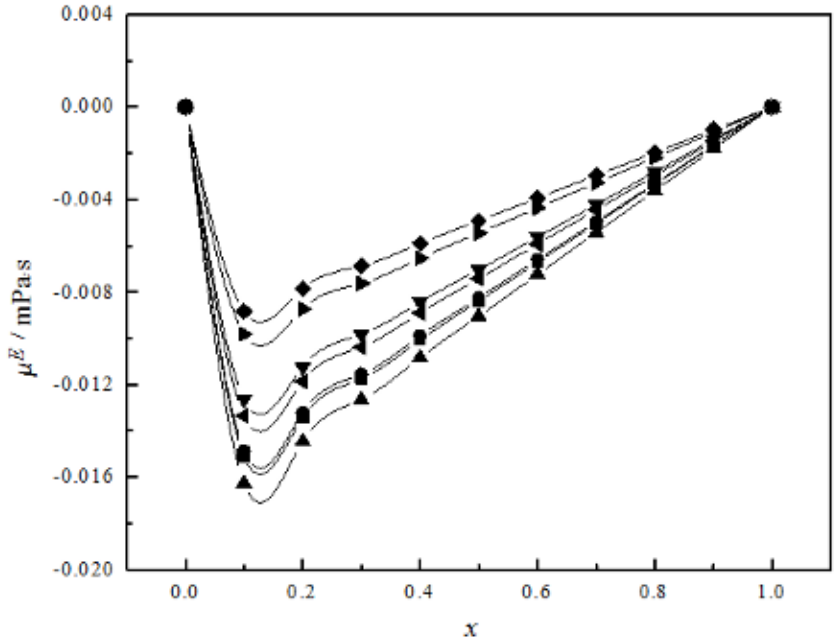

Figure 6. Plot of the excess viscosity data for the {TAPS (1) + H_2O (2)} system as a function of composition: ■, T_1 = 293.15 K ; ●, T_2 = 298.15 K; ▲, T_3 = 303.15 K; ▼, T_4 = 313.15 K; ◄, T_5 = 323.15 K; ►, T_6 = 333.15 K; ♦, T_7 = 343.15 K; and Lines are guide for the eyes.

IV. CONCLUSION

The densities, refractive indices, and viscosities of the aqueous solution of TAPS were reported for temperatures up to 343.15 K at atmospheric conditions. The measured properties were all found to decrease with temperature and increase with composition. A modified form of the Vogel-Tamman-Fulcher equation which leads to an Arrhenius-type asymptotic exponential function was used to correlate the temperature and compositional dependence of the considered properties. Satisfactory results were obtained as shown by an overall AAD value of 0.27%. Lastly, the excess properties were able to capture the non-ideal behavior upon mixing.

REFERENCES CITED

Civan F. 2008. Use of exponential functions to correlate temperature dependence. Chem. Eng. Prog. 104: 46-52.

De Jesus MB, Soriano AN, Li M-H. 2013. Thermophysical characterization of aqueous ternary system containing n-tris-[hydroxymethyl]methyl-3-amino propanesulfonic acid and glycol (PG or DPG or TPG). J. Chem. Thermodyn. 59: 80-86.

De Jesus MB, Soriano AN, Li M-H, Adornado AP. 2020. Densities of n-tris(hydroxymethyl)methyl-3-aminopropanesulfonic acid (TAPS) + glycol (DEG / TEG /T4EG) + water. IOP Conference Series: Earth and Envi. Sci. 471: 012007.

Geankoplis CJ. 1993. Transport Processes and Unit Operations. 3rd ed. Prentice-Hall International, Inc., Englewood Cliffs, New Jersey, U. S. A.

Graber TA, Galleguillos HR, Céspedes C, Taboada ME. 2004. Density, refractive index, viscosity, and electrical conductivity in the Na_2CO_3 + poly(ethylene glycol) + H_2O system from (293.15 to 308.15) K. J. Chem. Eng. Data 49: 1254-1257.

Transactions NAST PHL 43 (2021)
doi.org/10.57043/transnastphl.2021.1799

Gold Biotechnology. 2021. TAPS. https://www.goldbio.com/product/6731/taps; accessed December 26, 2021.

Machado CMM, Soares HMVM. 2007. Challenges in modelling and optimization of stability constants in the study of Cu–(TAPS)x–(OH)y system by polarography. Talanta 71: 1352-1363.

Machado CMM, Victoor O, Soares HMVM. 2007. Modelling of Pb–(TAPS)x–(OH)y system and refinement of stability constants in the region of lead hydrolysis and lead hydroxide precipitation. Talanta 71: 1326-1332.

NIST Chemistry WebBook. 2021. SRD 69, National Institute of Standards and Technology, U.S. Department of Commerce. https://webbook.nist.gov/chemistry/.

Palasz AT, Beltrán Breña P, De la Fuente J, Gutiérrez-Adán A. 2008. The effect of different zwitterionic buffers and PBS used for out-of-incubator procedures during standard in vitro embryo production on development, morphology and gene expression of bovine embryos. Theriogenology 70: 1461-1470.

Rooney D, Jacquemin J, Gardas R. 2009. Thermophysical Properties of Ionic Liquids. Ionic Liq. 290: 185-212.

Roy RN, Roy LN, LeNoue SR, Denton CE, Simon AN, Richards SJ, Moore AC, Roy CN, Redmond RR, Bryant PA. 2006. Thermodynamic constants of n-[tris(hydroxymethyl) methyl-3-amino]propanesulfonic acid (Taps) from the temperatures 278.15 K to 328.15 K. J. Chem. Thermodyn. 38: 413-417.

Schiebener P, Straub J. 1990. Refractive index of water and steam as function of wavelength, temperature and density. J. Phys. Chem. Ref. Data 19: 677-717.

Soriano AN, Cabahug DIV, Li M-H. 2011. Thermophysical property characterization of tris(hydroxymethyl)aminomethane. J. Chem. Thermodyn. 43: 186-189.

Taha M, Lee M-J. 2009a. Buffer interactions: Densities and solubilities of some selected biological buffers in water and in aqueous 1,4-dioxane solutions. Biochem. Eng. J. 46: 334-344.

Taha M, Lee M-J. 2009b. Interaction of biological buffers with electrolytes: Densities of aqueous solutions of two substituted aminosulfonic acids and ionic salts from T = (298.15 to 328.15) K. J. Chem. Thermodyn. 41: 705-715.

Taha M, Lee M-J. 2010a. Volumetric properties of MES, MOPS, MOPSO, and MOBS in water and in aqueous electrolyte solutions. Thermochim. Acta 505: 86-97.

Taha M, Lee M-J. 2010b. Buffer interactions: Solubilities and transfer free energies of TRIS, TAPS, TAPSO, and TABS from water to aqueous ethanol solutions. Fluid Phase Equilib. 289: 122-128.

Wong C-L, Soriano AN, Li M-H. 2008. Diffusion coefficients and molar conductivities in aqueous solutions of 1-ethyl-3-methylimidazolium-based ionic liquids. Fluid Phase Equilib. 271: 43-52.